

Electrochemical Performance of Ti-Si Alloy Anode using Nodule Type Current Collector

Min-Seon Shin, Jung-Bae Park, and Sung-Man Lee*

*Department of Nano Applied Engineering, Kangwon National University,
Chuncheon, Gangwon-Do, 200-701, South Korea*

(Received July 07, 2017 : Revised September 12, 2017 : Accepted September 14, 2017)

Abstract : The cycle performance of Ti-Si alloy anode material for Li-ion batteries has been investigated as a function of loading level of electrode using a nodule type of substrate, in which the current collector of flat foil is also used for comparison. The Ti-Si alloy powders are prepared by mechanical alloying method. The electrodes with the nodule type of current collector exhibit enhanced cycling performance compared to those using the flat foil because the alloy particles are more strongly adhered to substrate and the stress caused by lithiation and delithiation reaction can be effectively relaxed by nodule-type morphology. It appears, however, that the cycle performance is critically dependent on the loading level of electrode, even when the nodule type of current collector is applied. With high loading level, cracks are initiated at surface of electrode due to a steep stress gradient through the electrode thickness during cycling, leading to capacity fading.

Keywords : Si based alloys, Mechanical alloying, Current collector, Anode materials, Li-ion batteries

1. Introduction

Li-ion batteries are known as the preferred form of electrical energy storage system. Recently, an increase in energy density of Li-ion batteries is required. In this respect, Si has attracted attention because it has a high storage capacity (3572 mAh g^{-1} for $\text{Li}_{15}\text{Si}_4$) compared to commercial graphite having theoretical capacity of 372 mAh g^{-1} [1]. However, the practical application of Si anode is hindered due to poor cycle performance caused by the large volume changes ($\sim 300\%$) upon charging (lithiation) and discharging (delithiation). The large volume change of the Si active material can lead to the loss of electrical contact between active material particles or between active material particles and current collector. To overcome the large volume change and thus improve cycle performance of Si anodes, various approaches have been used. Most of the research has focused on the develop-

ment of new anode materials including Si nanostructures, Si alloys and Si/C composites [2-11].

On the other hand, the surface conditions of Cu current collector such as surface morphology also have a crucial role to play in dealing with the problem regarding the volume expansion in Si-based anodes [12-15]. Nevertheless, limited papers have paid attention to the effect of current collector on the cycle performance of Si-based electrodes prepared by slurry-coating [16,17]. A nodule-type Cu current collector appears to be effective in improving the cycle performance of Si-based anodes [16]. Moreover, it is very meaningful to investigate the effect of electrode thickness on the cycle performance of Si-based electrodes because the high loading level of the electrode is needed for lithium ion batteries with high energy density.

In this work, we demonstrate the morphology effect of Cu current collector on the cycle performance of Si alloy electrode with different loading levels. Electrochemical performance of Ti-Si alloy anodes using two types of Cu current collector, conventional flat and nodule-type, has been com-

*E-mail: smlee@kangwon.ac.kr

pared as a function of loading level of electrode.

2. Experimental

Mechanical alloying to prepare Ti-Si alloy was conducted for 3 h in a planetary mill with a water-cooling system using a hardened steel balls and vial, keeping ball to powder ratio of 10 : 1. Elemental Si (325 mesh, 98%) and titanium hydride (TiH_2) were used as starting materials. The mechanically alloyed Ti-Si sample shows two phases of Si and the metastable silicide (U-phase) [18]. This sample is designated in the text by the term MA Ti-Si.

For evaluation of the electrochemical characteristics, electrodes were fabricated by pasting an aqueous slurry containing 80 wt% active material, 10 wt% CB, and 10 wt% poly(acrylic acid) (PAA) on two types of copper foil of flat substrate and nodule-type substrate. The nodule-type Cu foil was obtained from Iljin Electrofoil Co., Ltd. The slurry-coated electrodes were then dried under vacuum at 180°C for 12 h and subsequently pressed. Coin cells with working electrodes and Li foil counter electrodes were assembled in an Ar-filled glove-box using 1 M LiPF_6 in a mixture of ethylene carbonate/diethyl carbonate (1:1 by volume) as the electrolyte. The cells were discharged (lithiated) and charged (delithiated) between 0.02 and 1.5 V (vs. Li/Li^+) at 30°C . Cells were discharged in constant current-constant voltage (CC-CV) mode (a constant current of 100 mA/g and then maintained at a constant voltage of 0.02 V) and charged at a constant current density of 100 mA/g for first the two cycles. After that, the electrodes were cycled in CC mode. Electrochemical impedance spectroscopy

(EIS) of electrodes after cycling was also performed in a frequency range of 1 MHz to 10 mHz with AC amplitude of 5 mV.

3. Results and Discussion

Fig. 1 a and b shows the cross-sectional SEM images of the MA Ti-Si electrodes coated on flat substrate and nodule-type substrate, respectively. With nodule-type substrate in comparison with flat substrate, it is considered that the contact area between coating layer and current collector is large and the composite coating layer is more strongly adhered to the substrate, in which some small active material (MA Ti-Si) particles can also be anchored between nodules.

Fig. 2 shows the cycle performance and coulombic efficiency of the MA Ti-Si electrodes coated on flat substrate and nodule-type substrate, in which the loading level for both electrodes was 4 mg cm^{-2} . The electrode with nodule-type foil displays better cycle performance than the electrode with flat foil. The former electrode maintains high coulombic efficiency of $\sim 99.8\%$ during cycling, while the latter electrode shows a relatively low coulombic efficiency of $\sim 99.3\%$. In general, the cycle performance of Si-based electrode is degraded mainly by the following two mechanisms: one is the electrical disconnection between active material particles or between active material particles and current collector and the other is the continuous formation of solid electrolyte interphase (SEI). The above mentioned failure mechanisms are associated with the large volume change of the Si phase during cycling. The volume contraction of the Si phase upon delithiation process results in a loss of electri-

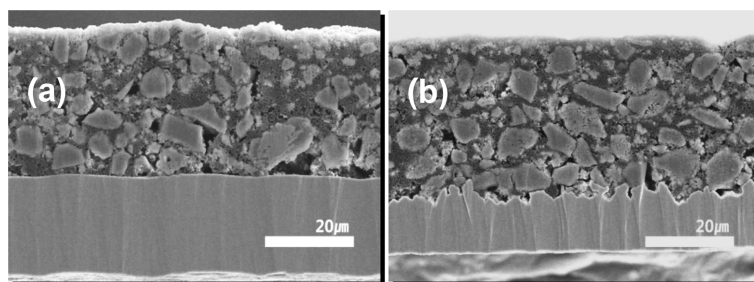


Figure 1. Cross-sectional SEM images of MA Ti-Si alloy electrodes on (a) flat and (b) nodule type substrate.

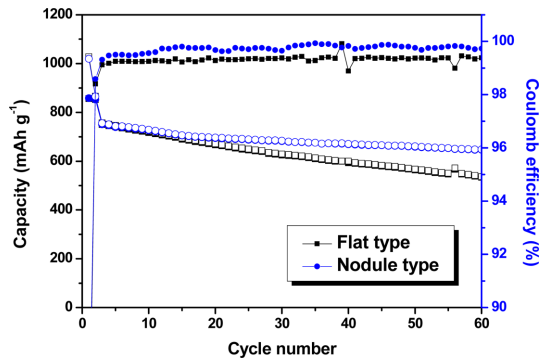


Figure 2. Cycle performance and coulombic efficiency of MA Ti-Si electrodes coated on flat and nodule type substrate.

cal connection in the electrode. The large repeated volume expansion/contraction can cause a failure of SEI layer of the Si-based electrode, resulting in continuous electrolyte decomposition and continuous formation of the SEI layer. Based on these considerations, the capacity retention of Si-based electrodes during cycling can be expressed in terms of cumulated relative irreversible capacities, in which the relative irreversible capacity (RIC) with cycling is defined as the ratio between the irreversible capacity loss and the delivered charge capacity [19]. The relative irreversible capacity associated with electrical disconnection and SEI formation is defined as follows [19]:

$$\text{RIC (disconn)} = (C_{c_n} - C_{c_{n+1}}) / C_{c_n} \quad (1)$$

where C_{c_n} is the charge capacity at cycle n and $C_{c_{n+1}}$ is charge capacity at cycle $n+1$.

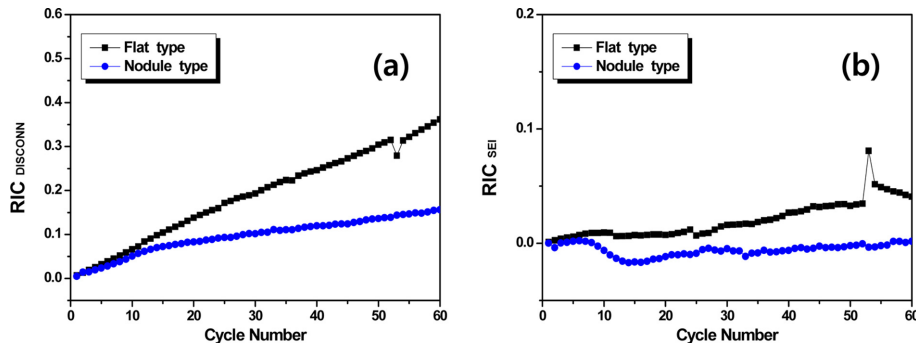


Figure 3. Relative irreversible capacity related to (a) disconnection (RIC(disconn)) and (b) SEI (RIC(SEI)) for MA Ti-Si alloy electrodes of flat and nodule type substrate.

$$\text{RIC(SEI)} = (C_{D_{n+1}} - C_{c_n}) / C_{c_n} \quad (2)$$

where $C_{D_{n+1}}$ is the discharge capacity at cycle $n+1$.

Fig. 3a and b shows the cumulated loss of RIC(disconn) and RIC(SEI) for both electrodes as a function of cycle, respectively. The irreversibility related to both of the electrical contact loss and SEI formation is significantly lower for nodule-type substrate electrode than that for flat substrate one. This is supported by the cross-sectional and surface SEM images after 20 cycles as shown in Fig. 4. For the electrode with flat substrate, the surface cracking proceeded markedly and the cracks propagated inward, while the surface cracking was not noticeable for nodule-type substrate although some internal cracks are visible (Fig. 4c). This indicates that the mechanical stability of the MA Ti-Si electrodes is significantly enhanced using the nodule-type substrate probably due to increased contact area and adhesion between coating layer and current collector.

On the other hand, even with the nodule-type substrate the cycling stability appears to be dependent on the loading level of the electrode. For the nodule-type substrate, the cycle performance of the electrodes, having two different loading levels of 4 mg cm^{-2} and 8 mg cm^{-2} , is compared (Fig. 5). No major difference can be observed between both electrodes until the 30th cycle. After that, the capacity decay with cycling is significantly higher in the case of the electrode with the higher loading level. Cross-sectional SEM images of the electrode with

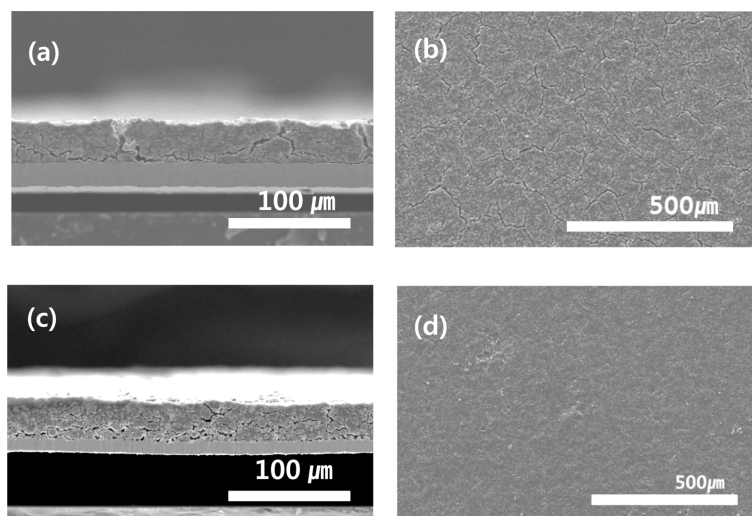


Figure 4. Cross sectional and surface SEM images of MA Ti-Si electrodes (a,b) flat and (c,d) nodule type substrate after 20 cycles.

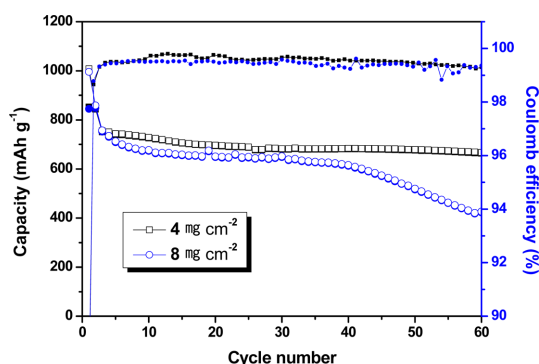


Figure 5. Cycle performance and coulombic efficiency of MA Ti-Si alloy electrodes on nodule type substrate with two different loading level of 4 mg cm^{-2} and 8 mg cm^{-2} .

the higher loading level reveal that cracks are found at the initial stages of cycling (only after 10 cycles), and the cracks initiate at the electrode surface as shown in Fig. 6(a). With increasing electrode thickness, the mass transport limitations of lithium ions in the electrolyte phase as well as the impedance for electrons in the solid phase of the electrode become dominating. Therefore, when the electrode is discharged and charged, MA Ti-Si particles in the upper region of the electrode are kinetically favored over those in the underlying regions. As a result, more lithium ions are inserted

into particles in the upper region than in the underlying regions and thus a stress gradient through the electrode thickness due to the volume changes of MA Ti-Si particles becomes steep, leading to an initiation of cracks at surface, while the particles are more strongly adhered to substrate and the stress can be effectively relaxed by nodule-type morphology. In contrast with the mechanical disintegration behavior of nodule-type electrode, in the case of flat substrate electrode having the loading level of 8 mg cm^{-2} , the coating layer was completely detached from the substrate after only 10 cycles as shown in Fig. 6(b).

The difference in cycle performance between nodule-type electrodes with different loading level is also confirmed by electrochemical impedance change with cycling. Fig. 7 compares the Nyquist plots of electrodes with two different loading levels of 4 mg cm^{-2} and 8 mg cm^{-2} after 20, 40 and 60 cycles. It should be noted that the specific impedance of the electrode was calculated based on the weight of active material per cm^2 of the electrode, i.e., weight specific impedance [20]. As shown in Fig. 7, both electrodes comprise one depressed semicircle in the high frequency range followed by a straight line portion in the low frequency range. The diameter of the depressed semicircle represents the overlap between the resistance of SEI

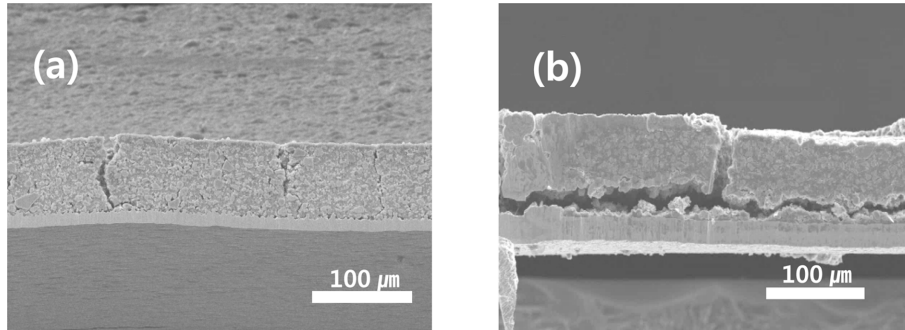


Figure 6. Cross sectional SEM images of MA Ti-Si alloy electrode on (a) nodule type substrate and (b) flat substrate with loading level of 8mg cm^{-2} .

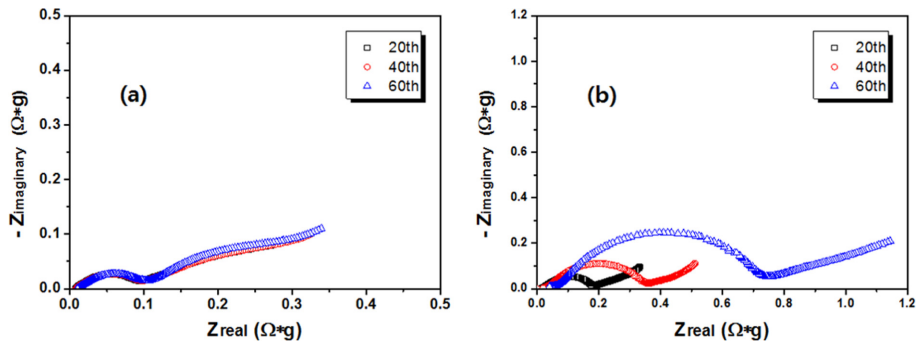


Figure 7. Nyquist plots of two electrodes on nodule type substrate with different loading level of (a) 4mg cm^{-2} and of (b) 8mg cm^{-2} .

layer and the charge-transfer resistance, and the straight line is related to the diffusion of lithium ion [21,22]. The electrode with low loading levels of 4mg cm^{-2} shows tiny variance in the cell resistance during 60 cycles, indicating that the MA Ti-Si electrode is maintaining stable interface impedance for lower loading levels. Meanwhile, the resistance of the electrode having high loading levels of 8mg cm^{-2} increases distinctly with cycling. As evidenced by SEM images (Fig. 4 and Fig. 6), the electrode with lower loading level keeps the structural integrity well after the repeated cycles, while the electrode with high loading level shows significant mechanical cracking. As more and more active material particles lose electrical contact with the active material particles and/or current collector on cycling, the impedance of the electrode increases as illustrated in Fig. 7. These results indicate that the performances of Si-based anodes can be effectively

enhanced only within a limited level of electrode loading even with well modified current collector like nodule-type foil. Above a critical thickness of coating layer, the crack is created by the volume changes of MA Ti-Si particles in the surface region of the electrode, which can cause splitting of the electrodes and lead to capacity fading upon prolonged cycling.

4. Conclusion

The electrodes coated on the nodule type substrate exhibited enhanced cycling performance compared to those coated on the flat foil. It is considered that the particles are more strongly adhered to substrate and the stress can be effectively relaxed by nodule-type morphology. However, the cycle performance is critically dependent on the loading level of electrode, even when the nodule

type substrate is applied. It appears that the performances of Si-based anodes can be effectively enhanced only within a limited level of electrode loading even with well modified current collector like nodule-type foil.

Acknowledgements

This work was supported by 2015 Research Grant from Kangwon National University (No. 520150036).

References

1. M. N. Obrovac, L. Christensen, D. B. Le, J. R. Dahn, 'Alloy Design for Lithium-Ion Battery Anodes' *J. Electrochem. Soc.*, 154, A849 (2007).
2. X. Su, Q. Wu, J. Li, X. Xiao, A. Lott, W. Lu, B. W. Sheldon, J. Wu, 'Silicon-Based Nanomaterials for Lithium Ion Batteries : A Review ' *Adv. Energy Mater.*, 4, 1300882 (2014).
3. W.-J. Zhang, 'A review of the electrochemical performance of alloy anodes for lithium-ion batteries' *J. Power Sources.*, 196, 13 (2011).
4. C.-M. Park, J.-H. Kim, H. Kim, H.-J. Shon, 'Li-alloy based anode materials for Li secondary batteries' *Chem. Soc. Rev.*, 39, 3115 (2010).
5. U. Kasavajjula, C. Wang, A. J. Appleby, 'Nano- and bulk-silicon-based insertion anodes for lithium-ion secondary cells' *J. Power Sources.*, 163, 1003 (2007).
6. H. Wu, Y. Cui, 'Designing nanostructured Si anodes for high energy lithium ion batteries' *Nano Today*, 7, 414 (2012).
7. Y. F. Gao, M. Cho, M. Zhou, 'Mechanical reliability of alloy-based electrode materials for rechargeable Li-ion batteries' *J. Mech. Sci. Technol.*, 27, 1205 (2013).
8. J. R. Szezech, S. Jin, 'Nanostructured silicon for high capacity lithium battery anodes' *Energy Environ. Sci.*, 4, 56 (2011).
9. H. Kim, B. Han, J. Choo, J. Cho, 'Three-dimensional porous silicon particles for use in high-performance lithium secondary batteries.' *Angew. Chem. Int. Ed.*, 47, 10151 (2008).
10. D. Larcher, S. Beattie, M. Morcrette, K. Edstrom, J.-C. Jumas, J.-M. Tarascon, 'Recent findings and prospects in the field of pure metals as negative electrodes for Li-ion batteries' *J. Mater. Chem.*, 17, 3759 (2007).
11. F. Luo, B. Liu, J. Zheng, G. Chu, K. Zhong, H. Li, X. Huang, L. Chen, 'Review—Nano-Silicon/Carbon Composite Anode Materials Towards Practical Application for Next Generation Li-Ion Batteries' *J. Electrochem. Soc.*, 162, A2509 (2015).
12. K. -L. Lee, J. -Y. Jung, S. -W. Lee, H. -S. Moon, J. -W. Park, 'Electrochemical characteristics of a-Si thin film anode for Li-ion rechargeable batteries' *J. Power Sources.*, 129, 270 (2004).
13. H. Guo, H. Zhao, C. Yin, W. Qju, 'A nanosized silicon thin film as high capacity anode material for Li-ion rechargeable batteries' *Mater. Sci. Eng. B.*, 131, 173 (2006).
14. T. Takamura, S. Ohara, M. Uehara, J. Suzuki, K. Sekine, 'A vacuum deposited Si film having a Li extraction capacity over 2000 mAh/g with a long cycle life' *J. Power Sources.*, 129, 96 (2004).
15. C. C. Nguyen, S. -W. Song, "Interfacial structural stabilization on amorphous silicon anode for improved cycling performance in lithium-ion batteries" *Electrochim. Acta.*, 55, 3026, (2010).
16. Y. -L. Kim, Y. -K. Sun, S. -M. Lee, "Enhanced electrochemical performance of silicon-based anode material by using current collector with modified surface morphology" *Electrochim. Acta.*, 53, 4500 (2008).
17. D. Reyter, S. Rousselot, D. Mazouzi, M. Gauthier, P. Moreau, B. Lestriez, D. Guyomard, L. Roue, "An electrochemically roughened Cu current collector for Si-based electrode in Li-ion batteries" *J. Power Sources.*, 239, 308 (2013). 308.
18. J. -B. Park, J. -S. Ham, M. -S. Shin, H. -K. Park, Y. -J. Lee, S. -M. Lee, "Synthesis and electrochemical characterization of anode material with titanium-silicon alloy solid core/nanoporous silicon shell structures for lithium rechargeable batteries" *J. Power Sources.*, 299, 537 (2015).
19. M. Gauthier, D. Mazouzi, D. Reyter, B. Lestriez, P. Moreau, D. Guyomard, L. Roue, "A low-cost and high performance ball-milled Si-based negative electrode for high-energy Li-ion batteries" *Energy Environ. Sci.*, 6, 2145 (2013).
20. H. Zheng, J. Li, X. Song, G. Liu, V. S. Battaglia, "A comprehensive understanding of electrode thickness effects on the electrochemical performances of Li-ion battery cathodes" *Electrochimica Acta.*, 71, 258 (2012).
21. J. C. Guo, X. L. Chen, C. S. Wang, "Carbon scaffold structured silicon anodes for lithium-ion batteries" *J. Mater. Chem.*, 20, 5035 (2010).
22. R. Ruffo, S. S. Hong, C. K. Chan, R. A. Huggins, Y. Cui, 'Impedance Analysis of Silicon Nanowire Lithium Ion Battery Anodes' *J. Phys. Chem. C.*, 113, 11390 (2009).